SM Higgs boson and $t \to cZ$ decays in the 2HDM type III with CP violation

R. Martinez*
Departamento de Física, Universidad Nacional de Colombia, K. 45 No. 26-85 Bogotá D.C., Colombia

R. Gaitán† and J. H. Montes de Oca‡
Departamento de Física, FES-Cuautitlán, UNAM, C.P. 54770 Estado de México, Mexico

E. A. Garcés§
Departamento de Física, Centro de Investigación y Estudios Avanzados del IPN, Apdo. Postal 14-740, 0700 Ciudad de México, Mexico

(Received 7 November 2017; published 21 August 2018)

We compute the contributions to rare top decays $t \to cZ$ and $t \to ch_1$ from the scalar sector in the two Higgs doublet model type III with CP violation, where h_1 is the Standard Model Higgs boson. The branching ratios for $\mathrm{BR}(t \to cZ)$ and $\mathrm{BR}(t \to ch_1)$ are obtained as a function of the model parameters. In particular, the $\mathrm{BR}(t \to cZ)$ can increase its value up to 10^{-3} for $\tan\beta = 1$ and masses for the additional Higgs bosons of $m_{h_2,h_3,H^\pm} \sim 0.5$ TeV. Meanwhile $\mathrm{BR}(t \to ch_1)$ can reach values of the order of $\sim 10^{-2}$. We constrain the model parameters (mixing angles of the neutral scalar fields in the CP violation context and $\tan\beta$) using the reported values of the signal strengths R_{XX} and $b \to s\gamma$ process.

DOI: 10.1103/PhysRevD.98.035031

I. INTRODUCTION

One of the goals of the Large Hadron Collider (LHC) was to observe the Higgs boson and look for physics beyond the Standard Model (SM). In 2012 the ATLAS and CMS collaborations took a big step with the observation of a SM-like Higgs boson with a mass of 125 GeV [1,2]; nevertheless, it was the first step in the long search of the Higgs boson from its theoretical assumption by the SM. This theory originally incorporated only one electroweak (EW) doublet scalar field where the Higgs boson particle arises when the symmetry $SU(2) \otimes U(1)$ is broken. Currently, there are no experimental and theoretical restrictions to suppose only one EW doublet scalar field, which suggests considering models with more scalar fields in order to study physics beyond the Standard Model (BSM). One of the simplest models reported in the literature is the two Higgs doublet model (2HDM) [3–11] which explains the hierarchy between the quark masses in the different families as a consequence of the hierarchy of vacuum expectation values (VEVs). The classification of the 2HDM is reviewed in detail in the report [12]. In the literature, usually the discrete symmetry Z_2 is used to control the couplings, and the models are classified according to their assignment of the values for the Z_2 charges in doublets and fermions. For instance, for the model named as 2HDM type I only one of the doublets gives masses to the fermions [13], while in the 2HDM type II both doublets participate in the masses of the fermions where each doublet is assigned to give mass to each fermion sector, respectively. One for the up and the other for the down sector [14]. Without this Z_2 symmetry both doublet scalar fields give masses to the up and down sectors (type III).

There are many motivations to extend the scalar sector of the SM. To understand the relic density of dark matter (DM) of the Universe, one possibility is the introduction of one scalar singlet which must have a VEV equal to zero. This is in order to avoid faster decay in SM particles and have the abundance according to the stellar dynamic and lensing effects [15–17].

Another possibility for the introduction of DM candidates is to add an EW doublet scalar field with VEV equal to zero; this model is known as the inert doublet model. Another interesting motivation for the extension of the scalar sector is the inclusion of CP violation in order to incorporate the matter-antimatter excess in the Universe [18–20].

Neutrino oscillations [21–23], transitions between different neutrino flavors ν_e, ν_μ, ν_τ, caused by nonzero neutrino

*remartinezm@unal.edu.co
†rgaitan@unam.mx
‡josehalim@comunidad.unam.mx
§estela.garces@gmail.com

masses, have been observed in the experiments with solar, atmospheric, reactor, and accelerator neutrinos [24–32]. The observation of neutrino oscillation requires the neutrino masses to be incorporated in the SM [33]. The neutrino masses can be generated through a seesaw mechanism. As a consequence, we have to introduce a unitarity matrix which relates the mass and flavor eigenstates. The diagonalization of the mass matrices of charged leptons and neutrinos generates the so-called Pontecorvo-Maki-Nakagawa-Sakata (PMNS) mixing matrix [21–23]. The PMNS matrix works similarly as the Cabibbo-Kobayashi-Maskawa (CKM) matrix, plus two additional CP phases for Majorana neutrinos. CP violation has been measured in the quark sector for the system $K^0 - \bar{K}^0$ and $B^0_{s(d)} - \bar{B}^0_{s(d)}$ [34–46]. On the other hand, long baseline neutrino experiments, such as NOvA, T2K, and Minos, could be observed CP violation in the neutrino sector [47,48].

The study of models with new sources of CP violation is very well motivated. In particular, the 2HDM type III, without including the Z_2 discrete symmetry, allows CP violation simultaneously in the scalar sector [49] and in the Yukawa Lagrangian. Under this assumption, the neutral CP-even and CP-odd Higgs bosons are combined in a scalar-pseudoscalar structure and their mass eigenstates do not have defined CP parity. The pseudoscalar coupling depends on the CP violation of the model, and it must be strongly suppressed.

Indirect evidence of a new physics signal in rare processes mediated by flavor-changing neutral currents (FCNC) could give a crucial direction to BSM physics [50,51]. The main motivation for considering FCNC is that these processes are extremely suppressed in the SM while their extensions are improved by FCNC approaching the experimental limits. The rare decays with FCNC, which have the greatest increase, are associated with the top quark such as $t \to qV$ for $q = u, c$ and $V = \gamma, g, Z$ [52–57]. The current experimental limit is yet 10 orders of magnitude apart from SM, the SM value is of the order of 10^{-17}–10^{-12} [52–57], and meanwhile the current experimental limits are $\mathrm{BR}(t \to q\gamma) < 5.9 \times 10^{-3}$ and $\mathrm{BR}(t \to qZ) < 2.1 \times 10^{-3}$ for $q = u, c$ [58]. In 2HDM with CP conserving the rare top decays present an increase in the branching ratio the order of 10^{-7}–10^{-9} [5–7,9,59–62]. This means that a signal of rare top decays near the LHC experimental limits will be clear evidence of new physics [63–70]. We analyze the flavor change (FC) in the context of 2HDM type III with CP violation which will introduce parameters, such as of α_1, α_2, α_3, and they are absent in the usual models. In order to find the allowed regions for $\{\alpha_1, \alpha_2, \tan\beta\}$ and Y_{tc}, we consider the contributions of the pseudoscalar couplings between the fermions and h_1 to R_{XX} by using the LHC measurements. Then we will find the values for the $\mathrm{BR}(t \to cZ)$ and $\mathrm{BR}(t \to ch_1)$ for this region of parameters.

The organization of the present work is the following. In Sec. II we present the model. In Sec. III we find the allowed region for the parameter space based on experimental values and χ^2 analysis. Section IV is devoted to presenting our results for the rare top decay. Finally, in Sec. V we discuss the obtained result and the perspectives for the model and in Sec. VI the conclusions.

II. MIXING AND FLAVOR-CHANGING NEUTRAL SCALARS IN 2HDM

Let us denote the two complex $SU(2)_L$ doublet scalar fields with hypercharge 1 as Φ_1 and Φ_2. If the $\Phi_{1,2}$ are included in the most general form in the Yukawa interactions and scalar potential, FC through neutral scalar fields can arise with the fermion interactions and general mixing for the three physical states of the neutral scalar. Usually, the discrete symmetry Z_2 is introduced in order to suppress these features in models with two doublet scalar fields. However, in the model considered in this work the Z_2 symmetry is avoided. This suppression is motivated by the experimental limits for FC processes; however, it could give signs of new physics and CP violation effects.

In the 2HDM type I or II, one of the Yukawa matrices is proportional to the mass fermion matrix which can be diagonalized by unitarity matrices as it happens in SM. By the other side, in the 2HDM type III the mass matrix for each fermion sector is a linear combination of both Yukawa matrices, which cannot be simultaneously diagonalized, and these new couplings, which arise from nondiagonal matrix elements, produce FC. In the scalar potential appear new bilinear and quartic interactions such as $\Phi_1^\dagger \Phi_2$ and $\Phi_1^\dagger \Phi_1 \Phi_1^\dagger \Phi_2$, which can induce CP violation explicitly. We study the 2HDM type III with explicit CP violation and flavor changing neutral scalar interaction (FCNSI), which is described below.

In the 2HDM type III the mixing of the neutral Higgs bosons, usually denoted as h^0, H^0, and A^0, follow closely the notation of Ref. [71]. The neutral Higgs bosons can be parametrized by the three angles $\{\alpha_1, \alpha_2, \alpha_3\}$, but in all decay channels of the lightest neutral Higgs boson, h_1, only α_1 and α_2 are required to describe the width decays. On the other hand, if $\alpha_2 = 0$, the mixing of the neutral Higgs bosons recover the CP parity and α_1 is the usual angle that mixes $h^0 - H^0$ in the CP-conserving 2HDM. The α_2 is an important parameter to analyze CP violation because when it is equal to zero all analytical expressions must be reduced to CP conserving 2HDM. Using the signal strengths, R_{XX}, reported by LHC [58] and predicted by 2HDM-III, we will find the allowed region for α_1, α_2, and $\tan\beta$, which is defined as a ratio of VEVs.

A. Yukawa interactions with FC

The most general structure for the Yukawa couplings among fermions and scalars is

$$\mathcal{L}_Y = \sum_{i,j=1}^{3}\sum_{a=1}^{2}(\bar{q}^0_{Li}Y^{0u}_{aij}\tilde{\Phi}_a u^0_{Rj} + \bar{q}^0_{Li}Y^{0d}_{aij}\Phi_a d^0_{Rj} + \bar{l}^0_{Li}Y^{0l}_{aij}\Phi_a e^0_{Rj} + \text{H.c.}), \quad (1)$$

where $Y^{u,d,l}_a$ are the 3×3 Yukawa matrices. q_L and l_L denote the left-handed fermion doublets under $SU(2)_L$, while u_R, d_R, l_R correspond to the right-handed singlets. The zero superscript in fermion fields and Yukawa matrices stands for the interaction basis and nondiagonal matrices in the most general case, respectively. The doublets are written as

$$\Phi_a = \begin{pmatrix} \phi^+_a \\ \phi^0_a \end{pmatrix}, \quad (2)$$

for $a = 1, 2$. The relation between the interaction and physical states is found through the spontaneous symmetry breaking (SSB), where the $U(1)_{\text{EM}}$-conserving VEVs can be taken as

$$\langle\Phi_1\rangle = \frac{1}{\sqrt{2}}\begin{pmatrix} 0 \\ v_1 \end{pmatrix}, \quad (3)$$

$$\langle\Phi_2\rangle = \frac{1}{\sqrt{2}}\begin{pmatrix} 0 \\ v_2 \end{pmatrix}, \quad (4)$$

where v_1 and v_2 are real and satisfy $v^2 \equiv v_1^2 + v_2^2$ with $v = \frac{2M_W}{g}$ [72]. After getting a correct SSB, Eqs. (3) and (4) are used in Eq. (1) to obtain the mass matrices, which are written as

$$M^{u,d,l} = \sum_{a=1}^{2}\frac{v_a}{\sqrt{2}}Y^{u,d,l}_a, \quad (5)$$

where $M^{u,d,l} = \text{diagonal}\{m_{u,d,e}, m_{c,s,\mu}, m_{t,b,\tau}\}$ and $Y^f_a = V^f_L Y^{0f}_a (V^f_R)^\dagger$, for $f = u, d, l$. The $V^f_{L,R}$ matrices are used to diagonalize the fermion mass matrices and to relate the physical and interaction states for fermions. Note that in 2HDM-III the diagonalization of mass matrices does not imply the diagonalization of the Yukawa matrices, as it occurs in the 2HDM type I or II. An important consequence of nondiagonal Yukawa matrices in physical states is the presence of FCNSI between neutral Higgs bosons and fermions.

We will only focus on the quarks; however, the charged leptons can be included in an analogous treatment. Equation (5) not only establish the mass matrices but also provide relations to eliminate one of the Yukawa matrices in the physical states. In order to obtain the interactions in terms of only one Yukawa matrix, Eq. (5) can be written in two possible forms,

$$Y^q_1 = \frac{\sqrt{2}}{v_1}M^q - \frac{v_2}{v_1}Y^q_2 \quad (6)$$

or

$$Y^q_2 = \frac{\sqrt{2}}{v_2}M^q - \frac{v_1}{v_2}Y^q_1, \quad (7)$$

where the quark sector label is $q = u, d$. The VEV's ratio defines the β parameter as $\frac{v_2}{v_1} = \tan\beta$, and then $v_1 = v\sin\beta$ and $v_2 = v\cos\beta$. By using Eq. (6) or Eq. (7) in the Yukawa Lagrangian $\mathcal{L}_Y$, Eq. (1), the 2HDM type III can be written in four different versions. For instance, from Eq. (7) we can find Y^u_2 and Y^d_2 as a function of the other Yukawa and masses obtaining

$$Y^u_2 = \frac{\sqrt{2}}{v_2}M^u - \frac{v_1}{v_2}Y^u_1, \qquad Y^d_2 = \frac{\sqrt{2}}{v_2}M^d - \frac{v_1}{v_2}Y^d_1. \quad (8)$$

Replacing them into Eq. (1), we obtain the Lagrangian 2HDM type I plus FC interactions. On the other hand, from Eqs. (6) and (7) we can also solve for

$$Y^u_2 = \frac{\sqrt{2}}{v_2}M^u - \frac{v_1}{v_2}Y^u_1, \qquad Y^d_1 = \frac{\sqrt{2}}{v_1}M^d - \frac{v_2}{v_1}Y^d_2. \quad (9)$$

Replacing them into Eq. (1), we obtain the Lagrangian 2HDM type II plus FC interactions. There are two other different 2HDM Lagrangians, and they are combinations of types I and II. They can be obtained by solving the Yukawas in the following form:

$$Y^u_1 = \frac{\sqrt{2}}{v_1}M^u - \frac{v_2}{v_1}Y^u_2, \qquad Y^d_1 = \frac{\sqrt{2}}{v_1}M^d - \frac{v_2}{v_1}Y^d_2, \quad (10)$$

and

$$Y^u_1 = \frac{\sqrt{2}}{v_1}M^u - \frac{v_2}{v_1}Y^u_2, \qquad Y^d_2 = \frac{\sqrt{2}}{v_2}M^d - \frac{v_1}{v_2}Y^d_1. \quad (11)$$

Taking into account similar rotations for the lepton sector there are only two Feynman rules which correspond to 2HDM types I and II plus FC. The general structure for the interactions between the quarks and neutral scalars in any of them is

$$\bar{q}[f(\beta)(A_L P_L + A_R P_R)M^q - g(\beta)(B_L P_L + B_R P_R)Y^q]qh_k, \quad (12)$$

where $P_{R,L} = \frac{1}{2}(1 \pm \gamma_5)$. The $f(\beta)$ or $g(\beta)$ can be written as sine, cosine, tangent, or cotangent of β, which will depend on the model version. The $A_{L,R}$ contain all the information related with the mixing of the neutral scalars h_k, which will be discussed below. The mass matrix must be diagonal; meanwhile, the Yukawa matrix could be, in general, nondiagonal. These elements of the Yukawa matrix are responsible for the FC mediated by neutral scalars.

B. Neutral scalar mixing from the scalar potential

Given Φ_1 and Φ_2 two complex $SU(2)_L$ doublet scalar fields, the most general gauge invariant and renormalizable Higgs scalar potential is [73,74]

$$\begin{aligned} V = {} & m_{11}^2\Phi_1^+\Phi_1 + m_{22}^2\Phi_2^+\Phi_2 - [m_{12}^2\Phi_1^+\Phi_2 + \text{H.c.}] \\ & + \frac{1}{2}\lambda_1(\Phi_1^+\Phi_1)^2 + \frac{1}{2}\lambda_2(\Phi_2^+\Phi_2)^2 + \lambda_3(\Phi_1^+\Phi_1)(\Phi_2^+\Phi_2) \\ & + \lambda_4(\Phi_1^+\Phi_2)(\Phi_2^+\Phi_1) + \frac{1}{2}\lambda_5((\Phi_1^+\Phi_2)^2 + (\Phi_2^+\Phi_1)^2) \\ & + [\lambda_6(\Phi_1^+\Phi_1)(\Phi_1^+\Phi_2) + \lambda_7(\Phi_2^+\Phi_2)(\Phi_1^+\Phi_2) + \text{H.c.}], \end{aligned} \tag{13}$$

where m_{11}^2, m_{22}^2 and λ_1, λ_2, λ_3, λ_4 are real parameters and meanwhile m_{12}^2, λ_5, λ_6, λ_7 can be complex parameters. The neutral components of the doublets, Eq. (2), in the interaction basis are $\phi_a^0 = \frac{1}{\sqrt{2}}(v_a + \eta_a + i\chi_a)$, where $a = 1, 2$. As a result of the explicit CP symmetry breaking introduced in Eq. (13), a mixing matrix R relates the mass eigenstates h_i with the η_i as follows:

$$h_i = \sum_{j=1}^{3} R_{ij}\eta_j. \tag{14}$$

Here, η_3 is the orthogonal state to the would-be Goldstone boson assigned to the Z gauge boson, and explicitly it is written as $\eta_3 = -\chi_1 \sin\beta + \chi_2\cos\beta$. The R matrix in Eq. (14) is parametrized in the usual form as [71]

$$R = \begin{pmatrix} c_1c_2 & s_1c_2 & s_2 \\ -(c_1s_2s_3 + s_1c_3) & c_1c_3 - s_1s_2s_3 & c_2s_3 \\ -c_1s_2c_3 + s_1s_3 & -(c_1s_3 + s_1s_2c_3) & c_2c_3 \end{pmatrix}, \tag{15}$$

where $c_i = \cos\alpha_i$, $s_i = \sin\alpha_i$ for $-\frac{\pi}{2} \le \alpha_{1,2} \le \frac{\pi}{2}$ and $0 \le \alpha_3 \le \frac{\pi}{2}$. h_i satisfy the mass relation $m_{h_1} \le m_{h_2} \le m_{h_3}$ [49,75–77]. In the CP-conserving case η_1 and η_2 are CP even and mixed in a 2×2 matrix while η_3 is CP odd decoupled from η_1 and η_2. However, because of CP-symmetry breaking, in general, the neutral Higgs bosons $h_{1,2,3}$ do not have well defined CP eigenstates. The CP-conserving limit is recovered when $\alpha_2 = \alpha_3 = 0$ [72]. In this case there is only mixing between the CP-even scalar fields.

The focus is on the up-type quark Yukawa interactions that contain the Feynman rules for the rare top decay. Replacing Eqs. (14) and (5) in the Yukawa Lagrangian of Eq. (1), the interactions between neutral Higgs bosons and fermions can be written as interactions of the CP-conserving 2HDM (type I or II) plus additional contributions, which arise from any of the $Y_{1,2}$ Yukawa matrices. The relation among the mass matrix M^f and the Yukawa matrices $Y_{1,2}^f$, for $f = u, d, l$, is used to write the Yukawa Lagrangian, Eq. (1), as a function of only one Yukawa matrix, Y_1^f or Y_2^f. We choose to write the interactions as a function of the Yukawa matrix Y_2, as follows:

$$Y_1^f = \frac{\sqrt{2}}{v_1}M^f - \frac{v_2}{v_1}Y_2^f. \tag{16}$$

We will replace Eq. (16) in Eq. (1) for $f = u, d$. From now on, in order to simplify the notation, the subscript 2 in the Yukawa couplings will be omitted. Therefore, the interactions between quarks and neutral scalar bosons are explicitly written as

$$\begin{aligned} \mathcal{L} = {} & \frac{1}{v\cos\beta}\sum_{ik}\bar{u}_iM^u(A_kP_L + A_k^*P_R)u_ih_k + \frac{1}{\cos\beta}\sum_{ijk}\bar{u}_iY_{ij}^u(B_kP_L + B_k^*P_R)u_jh_k \\ & \times\frac{1}{v\cos\beta}\sum_{ik}\bar{d}_iM^d(A_k^*P_L + A_kP_R)d_ih_k + \frac{1}{\cos\beta}\sum_{ijk}\bar{d}_iY_{ij}^d(B_k^*P_L + B_kP_R)d_jh_k \\ & + \frac{1}{v\cos\beta}\sum_{ik}\bar{e}_iM^l(A_k^*P_L + A_kP_R)e_ih_k + \frac{1}{\cos\beta}\sum_{ijk}\bar{e}_iY_{ij}^l(B_k^*P_L + B_kP_R)e_jh_k \\ & + \left[\frac{\sqrt{2}}{\cos\beta}\sum_{ij}\bar{u}_i((KY^d)_{ij}P_R - (Y^uK)_{ij}P_L)d_jH^+ \right. \\ & \left. + \frac{\sqrt{2}}{v}\tan\beta\sum_{ij}\bar{u}_i(-(KM^d)_{ij}P_R + (M^uK)_{ij}P_L)d_jH^+ + \text{H.c.}\right], \end{aligned} \tag{17}$$

where K is the CKM matrix and we define

$$\begin{aligned} A_k &= R_{k1} - iR_{k3}\sin\beta, \\ B_k &= R_{k2}\cos\beta - R_{k1}\sin\beta + iR_{k3}. \end{aligned} \tag{18}$$

The fermion spinors are denoted as $(u_1, u_2, u_3) = (u, c, t)$, where the indexes $i, j = 1, 2, 3$ denote the family generations in Eq. (17), while $k = 1, 2, 3$ is used for the neutral Higgs bosons. Note that a CP-conserving case is obtained only if two neutral Higgs bosons are mixed with well-defined CP states, for instance, if $\alpha_2 = \alpha_3 = 0$ is the usual limit [78].

In the CP-conserving limit, $\alpha_2 = \alpha_3 = 0$, the A_k and B_k coefficients are real parameters, for $k = 1, 2$, and meanwhile A_3 and B_3 are imaginary parameters. In this case, for the Lagrangian in Eq. (17) the CP-even and CP-odd Higgs couplings are scalar and pseudoscalar, respectively, which corresponds to the CP-conserving Lagrangian. The Y_{ij} coefficients, which produce FC, could be complex and their phases would introduce CP violation.

III. CONSTRAINTS FOR FC NEUTRAL SCALARS

Current observations in LHC impose restrictions on the neutral scalar h_1, which we will choose to be the SM Higgs boson. The strongest constraints for the $\alpha_{1,2}$ mixing angles come from its decay channels reported in the signal strength R_{XX} for fermions and gauge bosons in the final state [58]. The first part of this section (A) is devoted to finding bounds for $\tan\beta$ and charged Higgs mass using the measured $b \to s\gamma$ branching ratio. In the second part of this section (B), we perform a χ^2 analysis on R_{XX} with statistical errors only. We employ simultaneously R_{XX} and $b \to s\gamma$ to obtain allowed regions for the model parameters.

A. B physics constraints

The FC decay of the bottom quark $b \to s\gamma$ imposes the strongest constraint on $\tan\beta$. In the 2HDM this decay has a one loop contribution from charged and neutral Higgs bosons. We will use the reported value of $b \to s\gamma$ to constrain $\tan\beta$ and Yukawa matrix element Y_{tc}. In order to find allowed values for the parameters we first review the possible constraints that $b \to s\gamma$ decay can impose on the Y_{tc} coupling, assuming the charged Higgs in the range 500–900 GeV. New physics contributions can be parametrized in Wilson coefficients (WC). Following Refs. [79–83], the branching ratio of the $b \to s\gamma$ decay is a function of the WC. The main contributions due to Wilson coefficients, beyond the charged current contribution, are given by the charged Higgs and FC Yukawa couplings, $\delta C_{7,8} = C^{H^\pm_{7,8}} + C^{H,\mathrm{FC}}_{7,8}$. The charged-Higgs contribution is

$$C^{H^\pm_{7,8}} = \tan^2\beta(f^{(1)}_{7,8}(y_t) + f^{(2)}_{7,8}(y_t)), \tag{19}$$

while the FC contribution is

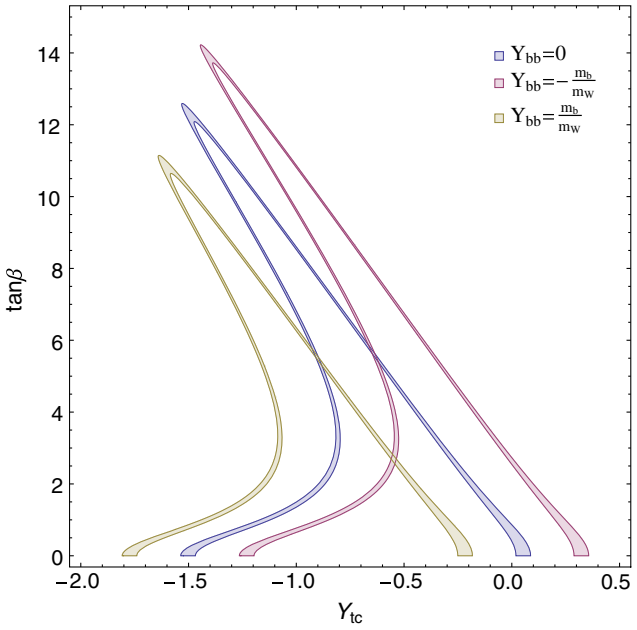

FIG. 1. $\tan\beta$ as a function of Y_{tc} considering different values of Y_{ff} and $m_{H^\pm} \approx 500$ GeV.

$$C^{H,\mathrm{FC}}_{7,8} = \frac{2M_W}{gm_t K_{ts}\cos\beta}(Y^u K)_{ts} f^{(1)}_{7,8}(y_t) + \frac{2M_W}{gm_b K_{tb}\cos\beta}(KY^d)_{tb} f^{(2)}_{7,8}(y_t), \tag{20}$$

with $y_t = m_t^2/M^2_{H^\pm}$, and the explicit relations for $f^{(1),(2)}_{7,8}(x)$ can be found in Refs. [79–83]. Using the hierarchy of the CKM matrix we have the following approximations: $(Y^u K)_{ts} \approx Y_{tc} K_{cs}$ and $(KY^d)_{tb} \approx K_{tb} Y_{bb}$. In order to bound the FC Yukawa coefficient Y_{tc}, we consider the Cheng-Sher Ansatz for Y_{bb} [11], meaning $Y_{ij} \approx \sqrt{m_i m_j}/m_W$, in particular, $Y_{bb} \approx m_b/m_W$. Limits on the $B \to X_s\gamma$ decay come from the B factory experiments *BABAR*, Belle, and CLEO [84–88]. The current HFAG world average for $E > 1.6$ GeV [89] is

$$\mathrm{BR}(B \to X_s\gamma) = (3.43 \pm 0.21 \pm 0.07) \times 10^{-4}. \tag{21}$$

In Fig. 1, the Cheng-Sher Ansatz for three different values of the Yukawa couplings Y_{bb} is considered to explore the allowed region in the $\tan\beta$-Y_{tc} plane. For $Y_{bb} = 0$ the allowed values for Y_{tc} are around the zero value which reproduced the results for 2HDM with CP conserving.

B. Constraints on the neutral scalar Higgs

The lightest neutral scalar h_1, Eq. (14), is assumed to be the SM scalar H^0 observed by ATLAS and CMS collaborations [1,2]. The measured signal strength R_{XX} for $X = b, W, Z, \tau, \gamma$ [58] (see Table I) can be used to constrain the parameter space in 2HDM. The signal strength for a given final state XX is

$$R_{XX} = \frac{\sigma \cdot \mathrm{BR}(H^0 \to XX)}{[\sigma \cdot \mathrm{BR}(H^0 \to XX)]_{\mathrm{SM}}}, \tag{22}$$

where H^0 is the observed Higgs in pp collisions at LHC, channel $pp \to gg \to h \to \gamma\gamma$. Similarly, we can define a signal strength for the new neutral boson h_1 in the 2HDM as

$$R_{XX}^{\mathrm{2HDM}} = \frac{[\sigma \cdot \mathrm{BR}(h_1 \to XX)]_{\mathrm{2HDM}}}{[\sigma \cdot \mathrm{BR}(H^0 \to XX)]_{\mathrm{SM}}}. \tag{23}$$

The 2HDM is constructed in such a way that the quark-gluon interactions remain as in the SM. Therefore, the R_{XX}^{2HDM} can be written only as the ratio of branching ratios of the 2HDM with charged-parity violation (CPV) and SM multiplied by the ratio between the decay width $h_1 \to gg$ and $H^0 \to gg$,

$$R_{XX}^{\mathrm{2HDM}} \approx \frac{\Gamma(h_1 \to gg)\mathrm{BR}(h_1 \to XX)}{\Gamma(H^0 \to gg)\mathrm{BR}(H^0 \to XX)}. \tag{24}$$

We will use the limits on R_{XX} reported by ATLAS and CMS to constrain the parameters in the model, by using Eq. (24).

The h_1 with a mass of the order of 125 GeV decays at tree level in the channel W^+W^-, ZZ, $f\bar{f}$; for $f = e, \mu, \tau, b, c, s, d$, meanwhile the channels at one loop are $\gamma\gamma$, γZ, gg. A model with CPV as the 2HDM type III also introduces a pseudoscalar coupling between neutral Higgs and fermions which also appears inside the loop in $h_1 \to \gamma\gamma, gg, \gamma Z$ through the top quark vertex. Since all fermions can give loop contributions since these contributions are proportional to the fermion masses, the top quark gives the greatest contribution. The decay widths in the 2HDM for $h_1 \to f\bar{f}$, with $f = b, c, s, u, d, \tau, \mu, e$, are given by

$$\Gamma_{h_1 \to f\bar{f}} = \frac{N_c m_{h_1}}{16\pi}\left(1 - 4\frac{m_f^2}{m_{h_1}^2}\right)^{\frac{1}{2}}\left[S_f^2\left(1 - 4\frac{m_f^2}{m_{h_1}^2}\right) + P_f^2\right], \tag{25}$$

where

$$\begin{aligned} S_f &= \frac{m_f}{v\cos\beta}R_{11} + Y_{ff}(R_{12} - R_{11}\tan\beta), \\ P_f &= -\frac{m_f \tan\beta}{v}R_{13} + \frac{Y_{ff}}{\cos\beta}R_{13}. \end{aligned} \tag{26}$$

P_f is the additional contribution coming from pseudoscalar coupling between Higgs and fermions due to CPV. For $\alpha_2 = 0$, $P_f = 0$. S_f is the usual 2HDM contribution. For $f = b$ the reported result can be revised in [91–98].

The Lagrangian used to calculate the Higgs decays at one loop level into $\gamma\gamma$, γZ, and gg is written as follows:

$$\begin{aligned} \mathcal{L} = &-\frac{gm_t}{2m_W}\bar{u}(t)(a_f + i\tilde{a}_f\gamma_5)u(t)h_1 + gm_W a_W W^+W^-h_1 \\ &+ \frac{1}{2}m_Z a_Z ZZh_1 - g\frac{m_{H^\pm}^2}{m_W}a_H H^+H^-h_1, \end{aligned} \tag{27}$$

where $a_{f,W,H}$ and $\tilde{a}_f$ are the deviations from the SM that are given by

$$\begin{aligned} a_f &= \frac{R_{11}}{\cos\beta} + \frac{Y_{tt}^u}{\cos\beta}\frac{2m_W}{gm_t}(R_{12}\cos\beta - R_{11}\sin\beta), \\ \tilde{a}_f &= \left(\sin\beta + \frac{Y_{tt}^u}{\cos\beta}\frac{2m_W}{gm_t}\right)R_{13}, \\ a_W &= a_Z = \cos\beta R_{11} + \sin\beta R_{12}, \\ a_H &= 1. \end{aligned} \tag{28}$$

It is important to note that if $\alpha_2 = 0$, then $\tilde{a}_f = 0$. In addition, the effect of considering $\alpha_2 = 0$ implies CP conserving. The three linear coupling in the charged and neutral Higgs bosons, $H^+H^-h_1$, can be approximated to $m_{H^\pm}^2$ in order to avoid the λ_i parameters from the Higgs potential. In this case, we assume the scalar coefficient as $a_H = 1$.

The partial width for the $h_1 \to \gamma\gamma$ decay is given by [99–107]

$$\begin{aligned} &\Gamma(h_1 \to \gamma\gamma) \\ &= \frac{G_F\alpha^2 m_{h_1}^3}{128\sqrt{2}\pi^3}\left[\left|\frac{4}{3}a_t A_{1/2}(\tau_t) + a_W A_1(\tau_W) + A_0(\tau_{H\pm})\right|^2 \right. \\ &\quad \left. + \left|\frac{8}{3}\tilde{a}_t\tilde{A}_{1/2}(\tau_t)\right|^2\right], \end{aligned} \tag{29}$$

where

$$\begin{aligned} A_1(\tau) &= 2 + 3\tau(2-\tau)f(\tau); \\ A_{1/2}(\tau) &= -2\tau[1 + (1-\tau)f(\tau)]; \\ \tilde{A}_{1/2}(\tau) &= \tau f(\tau); \\ A_0(\tau) &= [1 - \tau f(\tau)]; \end{aligned} \tag{30}$$

$\tau_i = \frac{4m_i^2}{m_{h_1}^2}$ for $i = t, W, H^\pm$; and

$$f(\tau) = \arcsin^2\left(\frac{1}{\sqrt{\tau}}\right). \tag{31}$$

Meanwhile for the $h_1 \to gg$ decay

$$\Gamma(h_1 \to gg) = \frac{G_F\alpha_s^2 m_{h_1}^3}{64\sqrt{2}\pi^3}[|a_t A_{1/2}(\tau_t)|^2 + |2\tilde{a}_t\tilde{A}_{1/2}(\tau_t)|^2]. \tag{32}$$

On the other hand, the width of $h_1 \to \gamma Z$ decay is [108–111]

$$\Gamma(h_1 \to \gamma Z) = \frac{G_F^2 \alpha m_W^2 m_{h_1}^3}{64\pi^4}\left(1-\frac{m_Z^2}{m_{h_1}^2}\right)^3 \times [|a_t B_{1/2}(\tau_t,\lambda_t) + a_W B_1(\tau_W,\lambda_W) + B_0(\tau_{H^\pm},\lambda_{H^\pm})|^2 + |\tilde{a}_t \tilde{B}_{1/2}(\tau_t,\lambda_t)|^2], \quad (33)$$

where

$$B_{1/2}(\tau,\lambda) = \frac{4(1-\frac{4}{3})}{\cos\theta_W}[I_1(\tau,\lambda) - I_2(\tau,\lambda)],$$
$$\tilde{B}_{1/2}(\tau,\lambda) = \frac{4(1-\frac{4}{3})}{\cos\theta_W} I_2(\tau,\lambda),$$
$$B_1(\tau,\lambda) = \cos\theta_W\left\{4(3-\tan^2\theta_W) I_2(\tau,\lambda) + \left[\left(1+\frac{2}{\tau}\right)\tan^2\theta_W - \left(5+\frac{2}{\tau}\right)\right] I_1(\tau,\lambda)\right\},$$
$$B_0(\tau,\lambda) = \frac{\cos 2\theta_W}{\cos\theta_W} I_1(\tau,\lambda), \quad (34)$$

and

$$I_1(\tau,\lambda) = \frac{\tau\lambda}{2(\tau-\lambda)} + \frac{\tau^2\lambda^2}{2(\tau-\lambda)^2}[f(\tau)-f(\lambda)] + \frac{\tau^2\lambda}{(\tau-\lambda)^2}[g(\tau)-g(\lambda)],$$
$$I_2(\tau,\lambda) = -\frac{\tau\lambda}{2(\tau-\lambda)}[f(\tau)-f(\lambda)], \quad (35)$$

with

$$g(\tau) = \sqrt{\tau-1}\arcsin^2\frac{1}{\sqrt{\tau}}, \quad (36)$$

and $\tau_i = \frac{4m_i^2}{m_{h_1}^2}$ for $i = t, W, H^\pm$. In Eqs. (29), (32), and (33), there is a term proportional to $\tilde{a}_t$ which represents the pseudoscalar coupling of the h_1 with $t\bar{t}$ at the loops. $\tilde{a}_t$ is proportional to $R_{13} = \sin\alpha_2$, which vanishes when the model is CP conserving.

For the $h_1 \to WW^*$, ZZ^* decays we will use the expressions reported in the literature [112]; however, these expressions must be multiplied by additional factors denoted by a_W^2 or a_Z^2 and they are given in Eq. (28), respectively, which arise from the 2HDM-III. Note that if the matrix elements R_{11}, R_{12}, and R_{13} are independent of the mixing parameter α_3 [see Eq. (15)], then all decays for h_1 do not depend on it. The CPV effects are only a function of α_1 and α_2.

In order to obtain the branching ratios for h_1, we calculate the partial widths for $b\bar{b}$, WW^*, ZZ^*, $c\bar{c}$, $\tau\bar{\tau}$, $\mu\bar{\mu}$ at tree level, and meanwhile gg, $\gamma\gamma$, γZ at one loop in the 2HDM type III. We note that the h_1 does not have well-defined CP parity and it couples to fermions with scalar and pseudoscalar interactions which contribute to partial width due to the Lagrangian Eq. (27). Similarly, the decays at one loop level with the top quark as an internal line in the loop will also have two contributions arising from scalar and pseudoscalar couplings. If the mixing angle $\alpha_2 = 0$, the pseudoscalar couplings vanish and the partial decay widths are reduced to the 2HDM with the CP-conserving case. The radiative corrections due to QCD, QED, and EW are considered in the numerical analysis from Refs. [90,113]. The masses of the fermions are also running to the scale of the SM boson mass ~125 GeV.

TABLE I. Reported values for R_{XX} and $\mathrm{BR}(H^0 \to XX)$ [58,90].

XX	R_{XX}^{exp}	$\mathrm{BR}(H^0 \to XX)$
$b\bar{b}$	0.82 ± 0.30	$5.84 \times 10^{-1}{}^{+3.2\%}_{-3.3\%}$
WW^*	$1.08^{+0.18}_{-0.16}$	$2.14 \times 10^{-1}{}^{+4.3\%}_{-4.2\%}$
gg	⋯	$7.3 \times 10^{-2}{}^{+3.61\%}_{-3.69\%}$
ZZ^*	$1.29^{+0.26}_{-0.23}$	$2.62 \times 10^{-2}{}^{+4.3\%}_{-4.1\%}$
$\tau\bar{\tau}$	1.12 ± 0.23	$6.27 \times 10^{-2}{}^{+5.7\%}_{-5.7\%}$
$\gamma\gamma$	1.16 ± 0.18	$2.27 \times 10^{-3}{}^{+5\%}_{-4.9\%}$
$c\bar{c}$	⋯	$5.1 \times 10^{-3}{}^{+5.5\%}_{-5.5\%}$
γZ	⋯	$1.53 \times 10^{-3}{}^{+9\%}_{-8.9\%}$
$\mu\bar{\mu}$	⋯	$2.18 \times 10^{-4}{}^{+6\%}_{-5.9\%}$

Following the measured at LHC of physical observables R_{bb}, R_{WW}, R_{ZZ}, $R_{\tau\tau}$, and $R_{\gamma\gamma}$ channels, we do a statistical analysis using a χ^2 function on the α_1, α_2, and $\tan\beta$ parameters for $m_{H^\pm} \approx 500$ GeV. To implement the χ^2 analysis we take into account the reported observables by ATLAS and CMS for R_{XX} shown in Table I. Figures 2–4 show the allowed values at 90% C.L. for the mixing parameters assuming fixed values of the Yukawa couplings.

The model with $\tan\beta = 0$ corresponds to one VEV equal to zero and its doublet is inert. However, in this case we have CPV couplings with fermion. For $\alpha_2 = 0$ the allowed regions for α_1 is $|\alpha_1| \lesssim 1.2$. We can see from Fig. 2 that the allowed region is consistent with $\alpha_1 = \alpha_2 = 0$, which corresponds to SM.

There is another interesting scenario in this model when $Y_{ff} \neq 0$. The Yukawa couplings Y_{ff} are restricted to be smaller than one in order to have a perturbative theory. These Yukawa couplings can be parametrized by the assumption of a certain structure or Ansatz that is motivated when some elements of the Yukawa matrix in the interaction basis are fixed to zero [114–129]. The Cheng-Sher Ansatz, $Y_{f_i f_j} \approx \frac{\sqrt{m_{f_i} m_{f_j}}}{m_W}$ [11], is also considered as limit values for Yukawa couplings in the chi^2 analysis. Figure 2

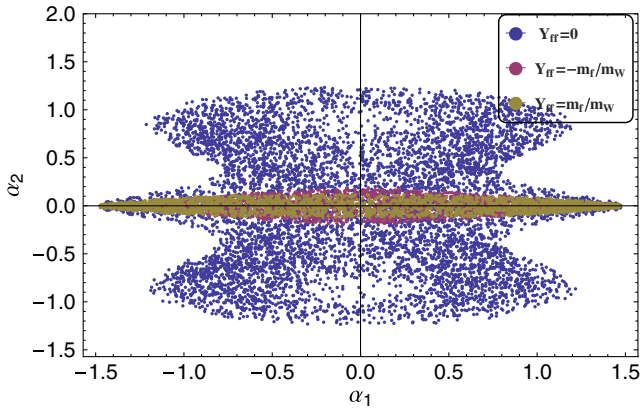

FIG. 2. Allowed regions for α_1 and α_2 with $Y_{ff}=0$ and $Y_{ff}=\pm\frac{m_f}{m_W}$, for $f=e,\mu,\tau,b,c,s,d$, obtained through χ^2 at 90% C.L. in R_{XX}.

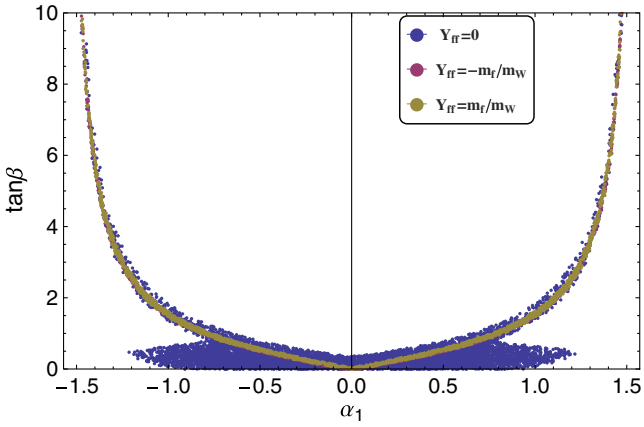

FIG. 3. Allowed regions for α_1 and $\tan\beta$ with $Y_{ff}=0$ and $Y_{ff}=\pm\frac{m_f}{m_W}$, for $f=e,\mu,\tau,b,c,s,d$, obtained through χ^2 at 90% C.L. in R_{XX}.

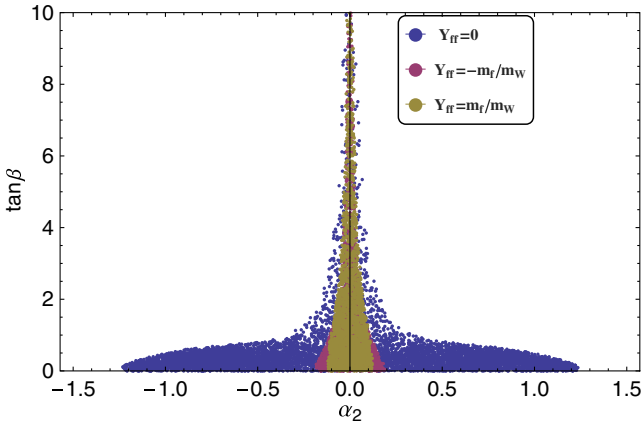

FIG. 4. Allowed regions for $\tan\beta$ and α_2 with $Y_{ff}=0$ and $Y_{ff}=\pm\frac{m_f}{m_W}$, for $f=e,\mu,\tau,b,c,s,d$, obtained through χ^2 at 90% C.L. in R_{XX}.

shows the allowed regions for α_1 and α_2 with Yukawa couplings fixed in the extreme values, $Y_{ff}=\frac{m_f}{m_W},-\frac{m_f}{m_W}$ and $Y_{ff}=0$. The last case, $Y_{ff}=0$, provides the greatest allowed region for mixing parameters.

The elements of the Yukawa matrices in Eq. (17) can be complex parameters in the most general case. However, the imaginary part of these couplings is strongly restricted by the electric dipole moment of the neutron [130]. In particular, restrictions over imaginary parts of the Yukawa couplings are obtained in the 2HDM with CP violation [131]. Nevertheless, in this work the Yukawa couplings are assumed to be real parameters and $Y_{ij}=Y_{ji}$.

In Figs. 3 and 4 we show regions in the planes α_1-$\tan\beta$ and α_2-$\tan\beta$, respectively, for fixed values of Yukawa couplings, and meanwhile Fig. 4 is for α_2 and $\tan\beta$. Note that $\alpha_2=0$ is a particular case of 2HDM without CPV. In this case Fig. 3 shows the values $\tan\beta>0$ and $|\alpha_1|\lesssim 1.5$ are preferred. On the other side, when $\alpha_2\neq 0$ the allowed region is reduced; for instance, in the case of $|\alpha_2|\gtrsim 0.2$ the allowed region is bounded by $\tan\beta<2$ as shown in Fig. 4.

IV. RARE TOP DECAYS

The observation of rare top decays with FCNC would be as a clear signal of physics beyond SM which can be understood in an extended model. We will analyze the rare top decays $t\to cZ$ and $t\to cH^0$ in this section, while the $t\to c\gamma$ and $t\to cg$ have been previously studied [63]. In the 2HDM type III, the neutral scalar field has a scalar and pseudoscalar coupling with the top quark that contributes inside the loop associated with the Higgs decay into two photons.

A. $t\to cZ$

The contributions from neutral scalars with FC to the amplitude for $t\to cZ$ decay are shown in Fig. 5. In general, the amplitude associated with the Feynman diagrams in Fig. 5 is written as

$$\mathcal{M}(t\to cZ)=\bar{u}(c)\Big[\gamma_\mu(V_LP_L+V_RP_R)+\frac{2i}{m_t}p_\mu(F_LP_L+F_RP_R)\Big]u(t)\epsilon_Z^\mu. \quad (37)$$

Here the q_μ contributions are not considered due to the gauge condition $\epsilon_Z\cdot q=0$. The form factors associated with γ_μ and p_μ can be related through the Gordon identity,

$$\frac{2ip_\mu}{m_t}P_{L,R}=\gamma_\mu P_{R,L}+\frac{i}{m_t}\sigma_{\mu\nu}q^\nu P_{L,R}. \quad (38)$$

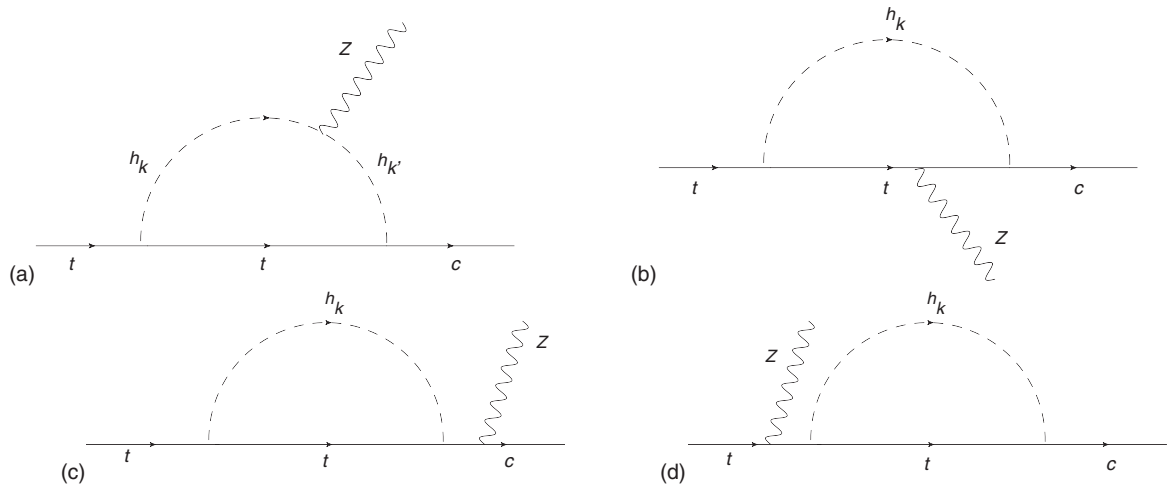

FIG. 5. Feynman diagrams for the $t \to cZ$ decay.

In the amplitude $\mathcal{M}(t \to cZ)$, the Gordon identity can be approximated as $\frac{2p_\mu}{m_t} P_{L,R} \approx \gamma_\mu P_{R,L}$, and the amplitude of $t \to cZ$ at one loop can be written as

$$\mathcal{M}(t \to cZ) = \frac{-i}{16\pi^2} \frac{g^2 m_t Y_{tc}}{M_W \cos\theta_W} \bar{u}(c) \sum_{D=a,b,c,d} \{\gamma_\mu [(\tilde{V}_L^D + \tilde{F}_R^D) P_L + (\tilde{V}_R^D + \tilde{F}_L^D) P_R]\} u(t) \epsilon_Z^\mu, \tag{39}$$

where $D = a, b, c, d$. The explicit values for all dimensionless form factors $\tilde{V}_{L,R}^D$ and $\tilde{F}_{L,R}^D$, after dimensional regularization, for Feynman diagrams are written in the Appendix. All contributions are finite because there is not a tcZ vertex at tree level and the Lagrangian cannot be renormalized. The amplitude in Eq. (39) is used to obtain

$$\Gamma(t \to cZ) = \frac{G_F^2 m_t^5 Y_{tc}^2}{256\pi^5} (1 - \hat{M}_Z^2)(1 + 2\hat{M}_Z^2)(|\tilde{A}|^2 + |\tilde{B}|^2), \tag{40}$$

where $\hat{M}_Z = \frac{M_Z}{m_t}$. The dimensionless terms $\tilde{A}$ and $\tilde{B}$ are

$$\tilde{A} = \sum_{D=a,b,c,d} (\tilde{V}_L^D + \tilde{F}_R^D), \tag{41}$$

$$\tilde{B} = \sum_{D=a,b,c,d} (\tilde{V}_R^D + \tilde{F}_L^D). \tag{42}$$

In order to obtain the branching ratio $\mathrm{BR}(t \to cZ)$ the SM width for the top quark can be approximated to the tbW width as [58]

$$\Gamma_{\text{top}} = \frac{G_f m_t^3}{8\pi\sqrt{2}} \left(1 - \frac{M_W^2}{m_t^2}\right)^2 \left(1 + 2\frac{M_W^2}{m_t^2}\right) \left[1 - \frac{2\alpha_s}{3\pi}\left(\frac{2\pi^2}{3} - \frac{5}{2}\right)\right]. \tag{43}$$

In the 2HDM-III with CPV, we include the FCNSI contributions, Eq. (40) in the total width for the top quark, such that $\Gamma_{\text{total}} = \Gamma_{\text{top}} + \Gamma_{\text{rare decays}}$, where $\Gamma_{\text{rare decays}} = \Gamma(t \to cZ) + \Gamma(t \to ch_1)$. The dominant contribution is the Γ_{top}; however, the $\Gamma_{\text{rare decays}}$ contribution, which contains $\Gamma(t \to ch_1)$ at tree level, can reach up to $\sim 1\%$ for specific values of the model parameters, as shown in the next subsection. When only the SM contribution is considered, the branching ratio for $t \to cZ$ can be approximated as

$$\mathrm{BR}(t \to cZ) \approx \frac{G_F^2 m_t^2 Y_{tc}^2}{16\sqrt{2}\pi^4} \frac{(1 - \hat{M}_Z^2)}{(1 - \hat{M}_W^2)} \frac{(1 + 2\hat{M}_Z^2)}{(1 + 2\hat{M}_W^2)} (|\tilde{A}|^2 + |\tilde{B}|^2). \tag{44}$$

The $|\tilde{A}|^2$ and $|\tilde{B}|^2$ are functions of the neutral scalar masses m_{h_k}, $k = 1, 2, 3$, and of the mixing parameters $\alpha_{1,2,3}$, β. h_1 is the SM Higgs mass, $m_{h_1} = 125$ GeV [58], and we fix the masses of the neutral scalars $h_{2,3}$ of the order of 600 GeV. The behavior of $\mathrm{BR}(t \to cZ)$ is shown in Figs. 6–8 in the following section.

B. $t \to cH$

In this subsection, we will analyze the FC top decay $t \to ch_1$ in this model, which can occur at tree level. The coupling for this decay is given in Eq. (17), and again the nonvanishing Y_{tc} is responsible for the flavor change through the neutral scalar mediation. The partial decay width is

$$\Gamma(t \to ch_1) = \frac{m_t}{8\pi} (1 - \hat{m}_{h_1}^2)^2 |Y_{tc}|^2 |B_1|^2, \tag{45}$$

where

$$B_1 = \cos\alpha_2 \cos(\alpha_1 - \beta) + i \sin\alpha_2 \tag{46}$$

is obtained from Eq. (13). Figures 9–11 show the behavior of this $\mathrm{BR}(t \to ch_1)$ as a function of the mixing parameters.

V. RESULTS AND DISCUSSION

We consider a model with explicit CP violation in the scalar sector, known as 2HDM-III. This model also contains neutral scalar fields that change flavor and have scalar-pseudoscalar interactions with the fermions, as we show in Eq. (17). This type of interaction is confronted with the current experimental results, for Higgs decays, through a χ^2 analysis. In this statistical analysis the following decay channels were taken into account: bb, $\gamma\gamma$, ZZ, WW, and $\tau\tau$. R_{XX} and the branching ratios were obtained in the 2HDM type III with CPV for h_1.

From the χ^2 analysis, allowed regions were found for mixing parameters with fixed values of Y_{ii}. The results are shown in Figs. 2–4. For large values of $\tan\beta$, it is shown that the allowed region is significantly suppressed, while in the opposite case, for small or zero values, the regions have a significant increase. This means that large values for $\tan\beta$, which can be considered from 10 approximately, are not viable to observe.

Two extreme cases were also considered for the Yukawa couplings, Y_{ff}. One of the cases was to assume $Y_{ff} = 0$, while the other case was to consider a maximum value determined by the Cheng-Sher parametrization. Under these assumptions a suppression was obtained when the Y_{ff} couplings participate, as shown in Figs. 3 and 4. The region that shows the greatest suppression is for α_2, which is bounded as $|\alpha_2| \lesssim 0.3$.

To study the behavior of the FC parameters, Y_{ij}, the reported value for the $b \to s\gamma$ was considered in an approximate scheme for its branching ratio expression in the 2HDM-III with CPV. Then, allowed values were obtained for Y_{tc} with different values $\tan\beta$ and Y_{bb} by assuming $m_{H^\pm} \approx 500$ GeV. In this scheme the charged Higgs contributes inversely proportional to $\tan\beta$, as it shows Eq. (19). The values obtained for Y_{tc} are shown in Fig. 1, which are used to analyze the $t \to cZ$ and $t \to ch_1$ decays in the 2HDM-III with CPV. In the $\Gamma(t \to cZ)$, we obtain the analytical expression at the loop level, Eq. (40), while for $\Gamma(t \to ch_1)$ the expression was calculated at tree level, Eq. (45), which are the highest contributions in the model.

In Fig. 7, we show $\mathrm{BR}(t \to cZ)$ as a function of α_1 for different values of $\tan\beta$. The $\mathrm{BR}(t \to cZ)$ for $Y_{ff} = 0$ can reach values of the order of 10^{-5}, while in the case $Y_{ff} = m_f/m_W$ the values increase to 8×10^{-4} for $\tan\beta = 1$.

The mixing angle α_2 was assigned with random values in the allowed region for SM Higgs and $b \to s\gamma$ decays. In Fig. 7, when we consider $Y_{ff} = 0$ and the value of α_1, in the allowed regions given by the Higgs decays and $bs\gamma$, the values for $\mathrm{BR}(t \to cZ)$ are between 10^{-7} and 10^{-5}; but in the limit when α_1 goes to zero, then $\mathrm{BR}(t \to cZ) \sim 10^{-9}$. On the other hand, when $Y_{ff} = m_f/m_W$, the values for $\mathrm{BR}(t \to cZ)$ are between 10^{-5} and 10^{-3}.

In Fig. 8, the behavior of $\mathrm{BR}(t \to cZ)$ as a function of α_2 is analogous to Fig. 7, but in these cases for α_2 allowed regions of the $\mathrm{BR}(t \to cZ)$ are not suppressed; in fact, the case of α_3 allows all the range and the greatest region for α_2. The α_3 is set as random values in the interval $[0, \pi/2]$ and the neutral Higgs masses $m_{h_2,h_3} \sim 500$ GeV.

For the $\mathrm{BR}(t \to ch_1)$, the results show a significant increase with respect to the results of $\mathrm{BR}(t \to cZ)$. For specific regions, as, e.g., $\tan\beta = 1$ and $Y_{ff} = m_f/m_W$, the $\mathrm{BR}(t \to ch_1)$ reaches a maximum value of the order 10^{-2}. Figure 12 shows a scatter plot considering these experimental limits and the allowed regions for the $\alpha_{1,2}$ parameters that correlate to the branching ratios for fixed values of $\tan\beta$ and Y_{ff}. This correlation shows a behavior such that $\mathrm{BR}(t \to cZ)$ is approximately 10^2–10^3 times lower

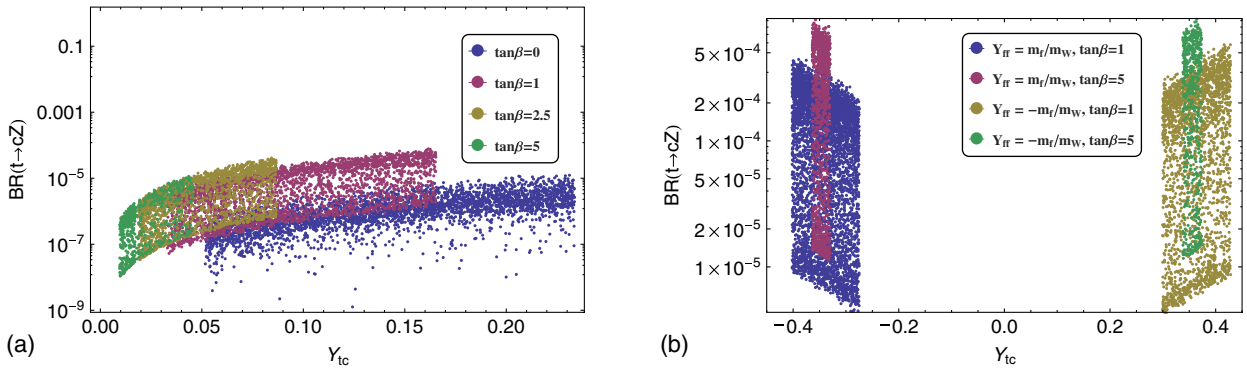

FIG. 6. $\mathrm{BR}(t \to cZ)$ as a function of Y_{tc} in the allowed regions for $\alpha_{1,2}$. (a) The behavior for $Y_{ff} = 0$. (b) Obtained when $Y_{ff} = \pm m_f/m_W$, $f = e, \mu, \tau, b, c, s, d$.

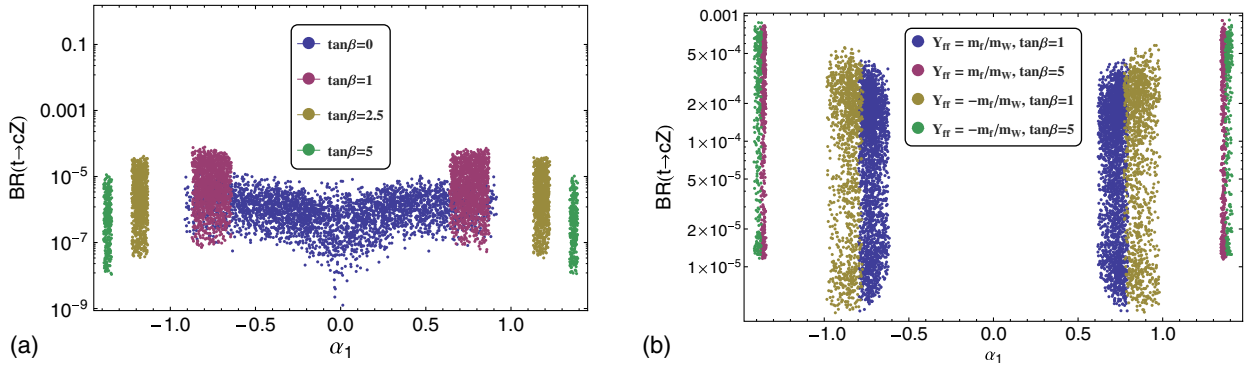

FIG. 7. $\mathrm{BR}(t \to cZ)$ as a function of α_1 for fixed values of $\tan\beta$ in the allowed regions for $\alpha_{1,2}$. (a) For $Y_{ff} = 0$. (b) For $Y_{ff} = \pm m_f/m_W$, for $f = e, \mu, \tau, b, c, s, d$.

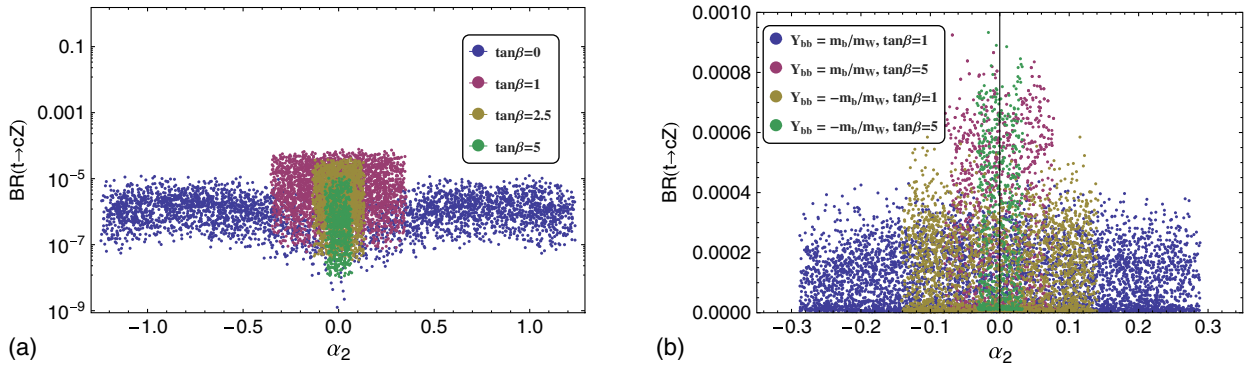

FIG. 8. $\mathrm{BR}(t \to cZ)$ as a function of α_2 for fixed values of $\tan\beta$ in the allowed regions for $\alpha_{1,2}$. (a) For $Y_{ff} = 0$. (b) For $Y_{ff} = \pm m_f/m_W$, for $f = e, \mu, \tau, b, c, s, d$.

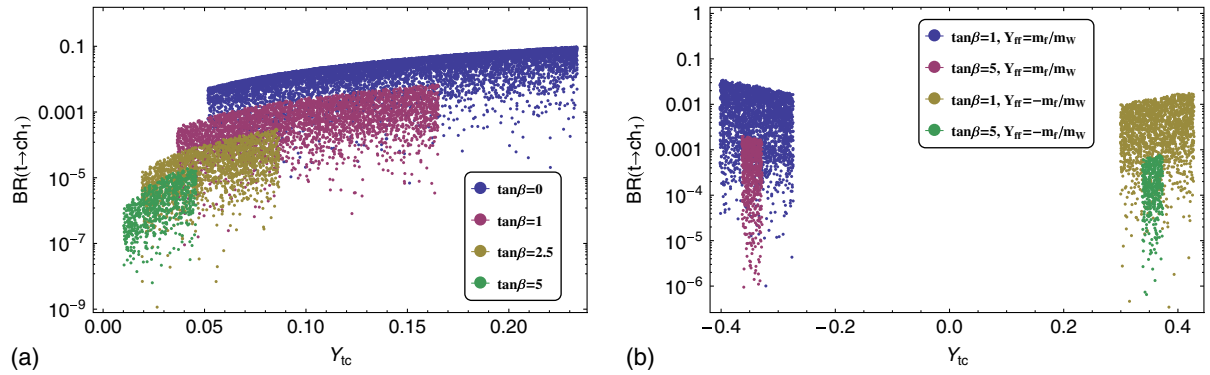

FIG. 9. $\mathrm{BR}(t \to ch_1)$ as a function of Y_{tc} for fixed values of $\tan\beta$ in the allowed regions for $\alpha_{1,2}$. (a) For $Y_{ff} = 0$. (b) For $Y_{ff} = \pm m_f/m_W$.

than $\mathrm{BR}(t \to ch_1)$. Figure 12 also shows that for $\tan\beta < 1$ the values of $\mathrm{BR}(t \to ch_1)$ are close to the reported limit, while for $Y_{ff} = m_f/m_W$ the values of the $\mathrm{BR}(t \to cZ)$ in the model are close to the experimental limit.

The experimental limits are $\mathrm{BR}(t \to cZ) < 3.7\%$ and $\mathrm{BR}(t \to cH^0) < 0.46\%$ [58]. We consider random values for the $\alpha_{1,2}$ parameters in the allowed regions at 90% C.L., obtained in Sec. III, to evaluate the $\mathrm{BR}(t \to cZ)$ and $\mathrm{BR}(t \to ch_1)$ in the 2HDM-III with CPV. The evaluation of these branching ratios has also been restricted by experimental limits. Figure 12 shows a scatter plot that correlates to $\mathrm{BR}(t \to cZ)$ and $\mathrm{BR}(t \to ch_1)$ for random values of $\alpha_{1,2,3}$ and Y_{tc} in the allowed regions when $\tan\beta$ is set.

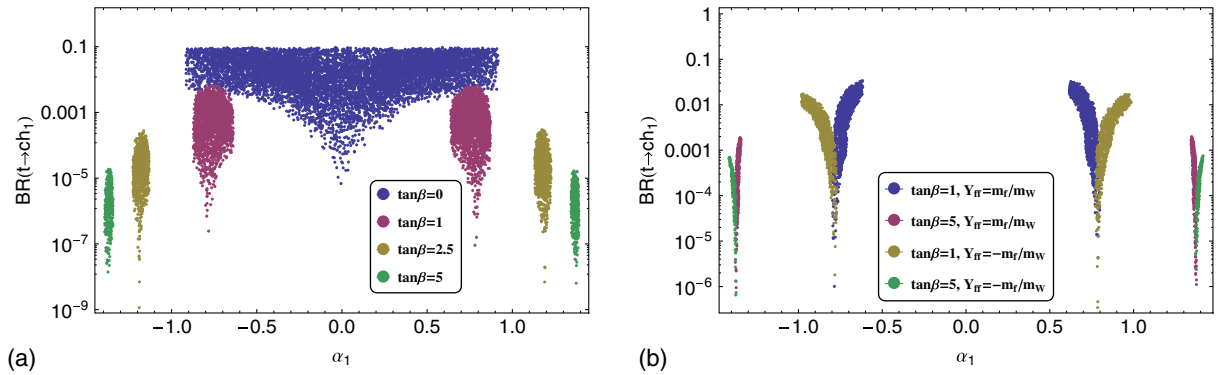

FIG. 10. $\mathrm{BR}(t \to ch_1)$ as a function of α_1 for fixed values of $\tan\beta$ in the allowed regions for $\alpha_{1,2}$. (a) For $Y_{ff} = 0$. (b) For $Y_{ff} = \pm m_f/m_W$.

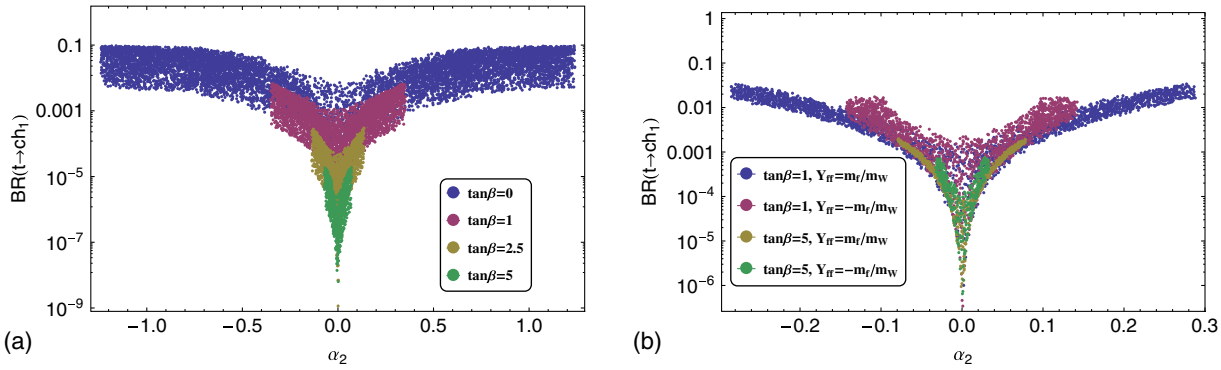

FIG. 11. $\mathrm{BR}(t \to ch_1)$ as a function of α_2 for fixed values of $\tan\beta$ in the allowed regions for $\alpha_{1,2}$. (a) For $Y_{ff} = 0$. (b) For $Y_{ff} = \pm m_f/m_W$, for $f = e, \mu, \tau, b, c, s, d$.

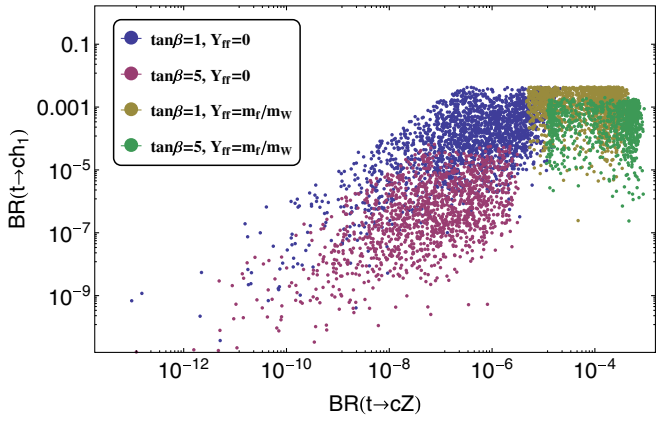

FIG. 12. Scatter plot of $\mathrm{BR}(t \to cZ)$ vs $\mathrm{BR}(t \to ch_1)$ for $\tan\beta = 1,\ 5$ and $Y_{ff} = 0, \pm m_f/m_W$, for $f = e, \mu, \tau, b, c, s, d$. We use random values for the allowed region in $\alpha_{1,2}$ found in the previous section.

VI. CONCLUSION

The FCNSI and explicit CP violation from the scalar sector are considered in a 2HDM when Yukawa couplings and the scalar potential are assumed in the most general form. We avoid including any discrete symmetry, such as the Z_2 symmetry. The model used in this work is classified as 2HDM type III with CP violation. The nondiagonal Yukawa couplings are responsible for the FCNSI; in particular, we study the contributions from the Y_{tc} element in the rare top decays $t \to cZ$ and $t \to ch_1$.

We obtain the analytical expressions for $\Gamma(t \to cZ)$ and $\Gamma(t \to ch_1)$ in the 2HDM type III with CPV at one loop and at tree level, respectively. Then, $\mathrm{BR}(t \to cZ)$ and $\mathrm{BR}(t \to ch_1)$ are analyzed in the allowed regions for α_1 and α_2 parameters with different fixed values of $\tan\beta$ and Yukawa couplings. These allowed regions are obtained by applying an χ^2 analysis at 90% C.L. into the Higgs decays. We also consider the contributions of 2HDM type III to $\mathrm{BR}(b \to s\gamma)$ with its experimental value to explore values of Y_{tc} as a function of Y_{bb} and $\tan\beta$ for $m_{H^\pm} \approx 500$ GeV. We find feasible scenarios for $\Gamma(t \to cZ)$ and $\Gamma(t \to ch_1)$ that can be comparable with the current experimental limits. For instance, the $\mathrm{BR}(t \to ch_1)$ can reach values of the order of 10^{-2} when $\Gamma(t \to cZ)$ is of the order of 10^{-4} for $\tan\beta = 1$ and $Y_{ff} = m_f/m_W$.

In Ref. [78] the couplings of the Higgs particle with a top and a light up-type quark u or c were written in Eq. (17). These couplings are responsible for the FCNC in the down-type Branco-Grimus-Lavoura (BGL) model and are functions of the α and β parameters. In the 2HDM

type III with CP violation the couplings of the Higgs particle with up-type quarks, denoted as $Y^u_{1,2}$, are free parameters. We can recover the $t \to c+$ Higgs decay rate in [78] when $\alpha_1 = \alpha$, $\alpha_2 = 0$, and $|Y_{tc}| = \frac{m_t}{2v}|V_{c\rho}||V_{t\rho}||t_\beta + t_\beta^{-1}|$ in 2HDM type III with CP violation. For instance, if $t_\beta = 2.5$, then $Y_{tc} = 0.043$ belongs to the allowed region in Fig. 9(a) in this work.

ACKNOWLEDGMENTS

This work was supported by projects Programa de Apoyo a Proyectos de Investigación e Innovación Tecnológica (PAPIIT) PAPIIT-IN113916 and PAPIIT-IA107118 in Dirección General de Asuntos de Personal Académico deUniversidad Nacional Autónoma de México (DGAPA-UNAM), programa interno de apoyo para proyectos de investigación (PIAPI) PIAPIVC07 in FES-Cuautitlán UNAM and *Sistema Nacional de Investigadores* (SNI) of the Consejo Nacional de Ciencia y Tecnología (CONACYT) in México. This work was supported by El Patrimonio Autonomo Fondo Nacional de Financiamiento para la Ciencia, la Tecnología y la Innovación Francisco José de Caldas programme of Departamento Administrativo de Ciencia, Tecnología e Innovación (COLCIENCIAS) in Colombia. J. H. M. is very grateful for the comments suggested by Omar G. Miranda to improve the analysis of this work.

APPENDIX: FORM FACTORS FOR $t \to cZ$ DECAY

The useful notation for masses is introduced as $\hat{x} = \frac{x}{m_t}$. Here, in order to simplify we introduce $\epsilon_{ij} = \frac{1}{2}(\sin\beta R_{i1}R_{k3} - \cos\beta R_{i2}R_{k3})$. After the dimensional regularization of the integrals for the $t \to cZ$ amplitude, we obtain for the Feynman diagrams $D = a, b, c, d$, shown in Fig. 5, the following results:

$$\tilde{V}_L^a = \int_0^1 dz \int_0^{1-z} dy \sum_{i\neq j} \epsilon_{ij}\left(A_i + \frac{vY_{tt}}{m_t}B_i\right)B_j^* \log(\hat{D}_1^2),$$
$$\tilde{V}_R^a = \int_0^1 dz \int_0^{1-z} dy \sum_{i\neq j} \epsilon_{ij}\left(A_i^* + \frac{vY_{tt}}{m_t}B_i^*\right)B_j \log(\hat{D}_1^2); \tag{A1}$$

$$\tilde{F}_L^a = \int_0^1 dz \int_0^{1-z} dy \sum_{i\neq j} \epsilon_{ij}\frac{1}{\hat{D}_1^2}\left[(y+z-1)y\left(A_i^* + \frac{vY_{tt}}{m_t}B_i^*\right)B_j - y\left(A_i + \frac{vY_{tt}}{m_t}B_i\right)B_j\right],$$
$$\tilde{F}_R^a = \int_0^1 dz \int_0^{1-z} dy \sum_{i\neq j} \epsilon_{ij}\frac{1}{\hat{D}_1^2}\left[(y+z-1)y\left(A_i + \frac{vY_{tt}}{m_t}B_i\right)B_j^* - y\left(A_i^* + \frac{vY_{tt}}{m_t}B_i^*\right)B_j^*\right]; \tag{A2}$$

$$\tilde{V}_L^b = \int_0^1 dz \int_0^{1-z} dy \sum_k \frac{1}{6\hat{D}_2^2}\left[[3+4s_W^2)\hat{D}_2^2 + (3-4s_W^2)(y+z-1)(y+z\hat{M}_Z^2) + 8s_W^2]\left(A_k + \frac{vY_{tt}}{m_t}B_k\right)B_k^*,\right.$$
$$\tilde{V}_R^b = \int_0^1 dz \int_0^{1-z} dy \sum_k \frac{1}{6\hat{D}_2^2}[4s_W^2\hat{D}_2^2 + 4s_W^2(y+z-1)(y+z\hat{M}_Z^2) + 2(3-4s_W^2)]\left(A_k^* + \frac{vY_{tt}}{m_t}B_k^*\right)B_k; \tag{A3}$$

$$\tilde{F}_L^b = \int_0^1 dz \int_0^{1-z} dy \sum_k \frac{1}{\hat{D}_2^2}\left[(3-4s_W^2)(y-1)A_kB_k^* - 4s_W^2(y+z-1)y\left(A_k^* + \frac{vY_{tt}}{m_t}B_k^*\right)B_k\right],$$
$$\tilde{F}_R^b = \int_0^1 dz \int_0^{1-z} dy \sum_k \frac{1}{\hat{D}_2^2}\left[4s_W^2(y-1)A_k^*B_k + (3-4s_W^2)2(y+z-1)y\left(A_k + \frac{vY_{tt}}{m_t}B_k\right)B_k^*\right]; \tag{A4}$$

$$\tilde{V}_L^c = \int_0^1 dz \int_0^{1-z} dy \sum_k \frac{1}{6}\log(\hat{D}_3^2)(3-4s_W^2)\left[z\left(A_k + \frac{vY_{tt}}{m_t}B_k\right)B_k^* + \left(A_k^* + \frac{vY_{tt}}{m_t}B_k^*\right)B_k\right],$$
$$\tilde{V}_R^c = \int_0^1 dz \int_0^{1-z} dy \sum_k \frac{1}{6}\log(\hat{D}_3^2)(-4s_W^2)\left[z\left(A_k^* + \frac{vY_{tt}}{m_t}B_k^*\right)B_k + \left(A_k + \frac{vY_{tt}}{m_t}B_k\right)B_k^*\right]; \tag{A5}$$

$$\tilde{V}_L^d = \int_0^1 dz \int_0^{1-z} dy \sum_k \frac{-1}{6}\log(\hat{D}_4^2)(3-4s_W^2)\left(A_k^* + \frac{vY_{tt}}{m_t}B_k^*\right)B_k^*,$$
$$\tilde{V}_R^d = \int_0^1 dz \int_0^{1-z} dy \sum_k \frac{1}{6}\log(\hat{D}_4^2)(4s_W^2)\left(A_k + \frac{vY_{tt}}{m_t}B_k\right)B_k; \tag{A6}$$

where

$$\hat{D}_1^2 = (1-\hat{M}_Z^2)yz + \hat{M}_Z^2 z^2 + (\hat{m}_j - \hat{m}_i - \hat{M}_Z^2)z + y^2 - \hat{m}_i^2 y + \hat{m}_i^2,$$
$$\hat{D}_2^2 = (1-\hat{M}_Z^2)yz + \hat{M}_Z^2(z^2 - z) + y^2(\hat{M}_Z^2 - 2)y + 1,$$
$$\hat{D}_3^2 == z^2 + (\hat{m}_k^2 - 2)z + 1,$$
$$\hat{D}_4^2 = (\hat{m}_k^2 - 1)z + 1. \tag{A7}$$

[1] G. Aad *et al.* (ATLAS Collaboration), Phys. Lett. B **716**, 1 (2012).
[2] S. Chatrchyan *et al.* (CMS Collaboration), Phys. Lett. B **716**, 30 (2012).
[3] J. F. Gunion, H. E. Haber, G. L. Kane, and S. Dawson, *The Higgs Hunter'S Guide* (Addison-Wesley, Reading, MA, 2000).
[4] S. L. Glashow and S. Weinberg, Phys. Rev. D **15**, 1958 (1977).
[5] D. Atwood, L. Reina, and A. Soni, Phys. Rev. Lett. **75**, 3800 (1995).
[6] G. Abbas, A. Celis, X. Q. Li, J. Lu, and A. Pich, J. High Energy Phys. 06 (2015) 005.
[7] D. Atwood, L. Reina, and A. Soni, Phys. Rev. D **53**, 1199 (1996).
[8] D. Atwood, L. Reina, and A. Soni, Phys. Rev. D **54**, 3296 (1996).
[9] D. Atwood, L. Reina, and A. Soni, Phys. Rev. D **55**, 3156 (1997).
[10] M. Sher and Y. Yuan, Phys. Rev. D **44**, 1461 (1991).
[11] T. P. Cheng and M. Sher, Phys. Rev. D **35**, 3484 (1987).
[12] G. C. Branco, P. M. Ferreira, L. Lavoura, M. N. Rebelo, M. Sher, and J. P. Silva, Phys. Rep. **516**, 1 (2012).
[13] H. E. Haber, G. L. Kane, and T. Sterling, Nucl. Phys. **B161**, 493 (1979).
[14] J. F. Donoghue and L. F. Li, Phys. Rev. D **19**, 945 (1979).
[15] J. McDonald, Phys. Rev. D **50**, 3637 (1994).
[16] J. McDonald, Phys. Rev. Lett. **88**, 091304 (2002).
[17] L. L. Honorez, E. Nezri, J. F. Oliver, and M. H. G. Tytgat, J. Cosmol. Astropart. Phys. 02 (2007) 028.
[18] A. D. Sakharov, Pis'ma Zh. Eksp. Teor. Fiz. **5**, 32 (1967) [JETP Lett. **5**, 24 (1967)]; Usp. Fiz. Nauk **161**, 61 (1991) [Sov. Phys. Usp. **34**, 392 (1991)].
[19] N. Cosme, L. L. Honorez, and M. H. G. Tytgat, Phys. Rev. D **72**, 043505 (2005).
[20] K. Fuyuto, W. Hou, and E. Senaha, Phys. Lett. B **776**, 402 (2018).
[21] B. Pontecorvo, Zh. Eksp. Teor. Fiz. **33**, 549 (1957) [Sov. Phys. JETP **6**, 429 (1957)].
[22] B. Pontecorvo, Zh. Eksp. Teor. Fiz. **34**, 247 (1957) [Sov. Phys. JETP **7**, 172 (1958)].
[23] Z. Maki, M. Nakagawa, and S. Sakata, Prog. Theor. Phys. **28**, 870 (1962).
[24] B. T. Cleveland, T. Daily, R. Davis, Jr., J. R. Distel, K. Lande, C. K. Lee, P. S. Wildenhain, and J. Ullman, Astrophys. J. **496**, 505 (1998).
[25] Y. Fukuda *et al.* (Kamiokande Collaboration), Phys. Rev. Lett. **77**, 1683 (1996).
[26] P. Anselmann *et al.* (GALLEX Collaboration), Phys. Lett. B **285**, 376 (1992).
[27] Q. R. Ahmad *et al.* (SNO Collaboration), Phys. Rev. Lett. **89**, 011301 (2002).
[28] S. Fukuda *et al.* (Super-Kamiokande Collaboration), Phys. Lett. B **539**, 179 (2002).
[29] K. Eguchi *et al.* (KamLAND Collaboration), Phys. Rev. Lett. **90**, 021802 (2003).
[30] T. Araki *et al.* (KamLAND Collaboration), Phys. Rev. Lett. **94**, 081801 (2005).
[31] Y. Fukuda *et al.* (Super-Kamiokande Collaboration), Phys. Rev. Lett. **81**, 1562 (1998).
[32] Y. Ashie *et al.* (Super-Kamiokande Collaboration), Phys. Rev. D **71**, 112005 (2005).
[33] C. D. Froggatt, M. Gibson, and H. B. Nielsen, Phys. Lett. B **409**, 305 (1997).
[34] Y. Grossman, Phys. Lett. B **380**, 99 (1996).
[35] I. Dunietz, R. Fleischer, and U. Nierste, Phys. Rev. D **63**, 114015 (2001).
[36] P. Langacker and M. Plumacher, Phys. Rev. D **62**, 013006 (2000).
[37] V. Barger, C. W. Chiang, P. Langacker, and H. S. Lee, Phys. Lett. B **580**, 186 (2004).
[38] S. Fajfer and P. Singer, Phys. Rev. D **65**, 017301 (2001).
[39] M. A. Perez and M. A. Soriano, Phys. Rev. D **46**, 284 (1992).
[40] D. L. Anderson and M. Sher, Phys. Rev. D **72**, 095014 (2005).
[41] J. A. Rodriguez and M. Sher, Phys. Rev. D **70**, 117702 (2004).
[42] C. Promberger, S. Schatt, and F. Schwab, Phys. Rev. D **75**, 115007 (2007).
[43] V. Barger, C. W. Chiang, J. Jiang, and P. Langacker, Phys. Lett. B **596**, 229 (2004).
[44] K. Cheung, C. W. Chiang, N. G. Deshpande, and J. Jiang, Phys. Lett. B **652**, 285 (2007).
[45] Y. Grossman, Y. Nir, and G. Raz, Phys. Rev. Lett. **97**, 151801 (2006).
[46] R. Martinez and F. Ochoa, Phys. Rev. D **77**, 065012 (2008).
[47] P. Adamson *et al.* (NOvA Collaboration), Phys. Rev. Lett. **116**, 151806 (2016).
[48] M. C. Gonzalez-Garcia and M. Maltoni, Phys. Rep. **460**, 1 (2008).

[49] L. Basso, A. Lipniacka, F. Mahmoudi, S. Moretti, P. Osland, G. M. Pruna, and M. Purmohammadi, J. High Energy Phys. 11 (2012) 011.
[50] M. Lindner, M. Platscher, and F. S. Queiroz, Phys. Rep. **731**, 1 (2018).
[51] L. J. Hall and M. B. Wise, Nucl. Phys. **B187**, 397 (1981).
[52] G. Eilam, J. L. Hewett, and A. Soni, Phys. Rev. D **44**, 1473 (1991); **59**, 039901(E) (1998).
[53] J. A. Aguilar-Saavedra and B. M. Nobre, Phys. Lett. B **553**, 251 (2003).
[54] J. A. Aguilar-Saavedra, Acta Phys. Pol. B **35**, 2695 (2004).
[55] B. Mele, S. Petrarca, and A. Soddu, Phys. Lett. B **435**, 401 (1998).
[56] J. L. Diaz-Cruz, R. Martinez, M. A. Perez, and A. Rosado, Phys. Rev. D **41**, 891 (1990).
[57] F. Larios, R. Martinez, and M. A. Perez, Int. J. Mod. Phys. A **21**, 3473 (2006).
[58] C. Patrignani *et al.* (Particle Data Group), Chin. Phys. C **40**, 100001 (2016).
[59] B. Grzadkowski, J. F. Gunion, and P. Krawczyk, Phys. Lett. B **268**, 106 (1991).
[60] A. Arhrib, Phys. Rev. D **72**, 075016 (2005).
[61] S. Bejar, J. Guasch, and J. Sola, Nucl. Phys. **B600**, 21 (2001).
[62] M. E. Luke and M. J. Savage, Phys. Lett. B **307**, 387 (1993).
[63] R. Gaitán, J. H. Montes de Oca, E. A. Garcés, and R. Martinez, Phys. Rev. D **94**, 094038 (2016).
[64] A. Diaz-Furlong, M. Frank, N. Pourtolami, M. Toharia, and R. Xoxocotzi, Phys. Rev. D **94**, 036001 (2016).
[65] H. Hesari, H. Khanpour, and M. M. Najafabadi, Phys. Rev. D **92**, 113012 (2015).
[66] T. Enomoto and R. Watanabe, J. High Energy Phys. 05 (2016) 002.
[67] U. K. Dey and T. Jha, Phys. Rev. D **94**, 056011 (2016).
[68] S. Khatibi and M. M. Najafabadi, Nucl. Phys. **B909**, 607 (2016).
[69] R. Gaitan, J. H. Montes de Oca, and J. A. Orduz-Ducuara, Prog. Theor. Exp. Phys. **2017**, 073B02 (2017).
[70] D. Bardhan, G. Bhattacharyya, D. Ghosh, M. Patra, and S. Raychaudhuri, Phys. Rev. D **94**, 015026 (2016).
[71] A. W. El Kaffas, W. Khater, O. M. Ogreid, and P. Osland, Nucl. Phys. **B775**, 45 (2007).
[72] I. F. Ginzburg and M. Krawczyk, Phys. Rev. D **72**, 115013 (2005).
[73] H. E. Haber and R. Hempfling, Phys. Rev. D **48**, 4280 (1993).
[74] X. J. Xu, Phys. Rev. D **95**, 115019 (2017).
[75] A. Arhrib, E. Christova, H. Eberl, and E. Ginina, J. High Energy Phys. 04 (2011) 089.
[76] M. Krawczyk, D. Sokolowska, P. Swaczyna, and B. Swiezewska, J. High Energy Phys. 09 (2013) 055.
[77] C. Y. Chen, S. Dawson, and Y. Zhang, J. High Energy Phys. 06 (2015) 056.
[78] F. J. Botella, G. C. Branco, M. Nebot, and M. N. Rebelo, Eur. Phys. J. C **76**, 161 (2016).
[79] G. Degrassi, P. Gambino, and G. F. Giudice, J. High Energy Phys. 12 (2000) 009.
[80] M. Misiak *et al.*, Phys. Rev. Lett. **98**, 022002 (2007).
[81] E. Lunghi and J. Matias, J. High Energy Phys. 04 (2007) 058.
[82] M. E. Gomez, T. Ibrahim, P. Nath, and S. Skadhauge, Phys. Rev. D **74**, 015015 (2006).
[83] G. Barenboim, C. Bosch, M. L. Lopez-Ibañez, and O. Vives, J. High Energy Phys. 11 (2013) 051.
[84] S. Chen *et al.* (CLEO Collaboration), Phys. Rev. Lett. **87**, 251807 (2001).
[85] K. Abe *et al.* (Belle Collaboration), Phys. Lett. B **511**, 151 (2001).
[86] J. P. Lees *et al.* (*BABAR* Collaboration), Phys. Rev. D **86**, 052012 (2012).
[87] J. P. Lees *et al.* (*BABAR* Collaboration), Phys. Rev. D **86**, 112008 (2012).
[88] B. Aubert *et al.* (*BABAR* Collaboration), Phys. Rev. D **77**, 051103 (2008).
[89] Y. Amhis *et al.* (Heavy Flavor Averaging Group (HFAG)), arXiv:1412.7515.
[90] D. de Florian *et al.* (LHC Higgs Cross Section Working Group), arXiv:1610.07922.
[91] B. A. Kniehl and M. Spira, Nucl. Phys. **B432**, 39 (1994).
[92] A. Djouadi, M. Spira, and P. M. Zerwas, Z. Phys. C **70**, 427 (1996).
[93] K. G. Chetyrkin and A. Kwiatkowski, Nucl. Phys. **B461**, 3 (1996).
[94] S. A. Larin, T. van Ritbergen, and J. A. M. Vermaseren, Phys. Lett. B **362**, 134 (1995).
[95] K. Melnikov, Phys. Rev. D **53**, 5020 (1996).
[96] K. G. Chetyrkin, Phys. Lett. B **390**, 309 (1997).
[97] M. Spira, Prog. Part. Nucl. Phys. **95**, 98 (2017).
[98] A. Kwiatkowski and M. Steinhauser, Phys. Lett. B **338**, 66 (1994); **342**, 455(E) (1995).
[99] A. Djouadi, Phys. Rep. **457**, 1 (2008).
[100] M. Spira, A. Djouadi, D. Graudenz, and P. M. Zerwas, Nucl. Phys. **B453**, 17 (1995).
[101] M. Spira, A. Djouadi, D. Graudenz, and P. M. Zerwas, Phys. Lett. B **318**, 347 (1993).
[102] A. Djouadi, M. Spira, J. J. van der Bij, and P. M. Zerwas, Phys. Lett. B **257**, 187 (1991).
[103] A. Djouadi, M. Spira, and P. M. Zerwas, Phys. Lett. B **311**, 255 (1993).
[104] Y. Liao and X. y. Li, Phys. Lett. B **396**, 225 (1997).
[105] R. Martinez, M. A. Perez, and J. J. Toscano, Phys. Rev. D **40**, 1722 (1989).
[106] R. Martinez, M. A. Perez, and J. J. Toscano, Phys. Lett. B **234**, 503 (1990).
[107] R. Martinez and M. A. Perez, Nucl. Phys. **B347**, 105 (1990).
[108] M. Spira, A. Djouadi, and P. M. Zerwas, Phys. Lett. B **276**, 350 (1992).
[109] M. Spira, Fortschr. Phys. **46**, 203 (1998).
[110] G. A. Gonzalez-Sprinberg, R. Martinez, and J. A. Rodriguez, Phys. Rev. D **71**, 035003 (2005).
[111] A. Cordero-Cid, J. Hernandez-Sanchez, C. G. Honorato, S. Moretti, M. A. Perez, and A. Rosado, J. High Energy Phys. 07 (2014) 057.
[112] W. Y. Keung and W. J. Marciano, Phys. Rev. D **30**, 248 (1984).
[113] A. Dabelstein and W. Hollik, Z. Phys. C **53**, 507 (1992).
[114] D. S. Du and Z. z. Xing, Phys. Rev. D **48**, 2349 (1993).

[115] L. J. Hall and A. Rasin, Phys. Lett. B **315**, 164 (1993).
[116] H. Fritzsch and D. Holtmannspotter, Phys. Lett. B **338**, 290 (1994).
[117] H. Fritzsch and Z. z. Xing, Phys. Lett. B **353**, 114 (1995).
[118] H. Fritzsch and Z. z. Xing, Phys. Lett. B **413**, 396 (1997).
[119] H. Fritzsch and Z. z. Xing, Phys. Rev. D **57**, 594 (1998).
[120] H. Fritzsch and Z. z. Xing, Nucl. Phys. **B556**, 49 (1999).
[121] G. C. Branco, D. Emmanuel-Costa, and R. Gonzalez Felipe, Phys. Lett. B **477**, 147 (2000).
[122] R. Rosenfeld and J. L. Rosner, Phys. Lett. B **516**, 408 (2001).
[123] J. L. Chkareuli, C. D. Froggatt, and H. B. Nielsen, Nucl. Phys. **B626**, 307 (2002).
[124] H. Fritzsch and Z. z. Xing, Phys. Lett. B **555**, 63 (2003).
[125] K. Matsuda and H. Nishiura, Phys. Rev. D **74**, 033014 (2006).
[126] Y. Koide, H. Nishiura, K. Matsuda, T. Kikuchi, and T. Fukuyama, Phys. Rev. D **66**, 093006 (2002).
[127] K. Matsuda and H. Nishiura, Phys. Rev. D **69**, 053005 (2004).
[128] A. E. Carcamo Hernandez, R. Martinez, and F. Ochoa, Phys. Rev. D **73**, 035007 (2006).
[129] A. Crivellin, A. Kokulu, and C. Greub, Phys. Rev. D **87**, 094031 (2013).
[130] J. Brod, U. Haisch, and J. Zupan, J. High Energy Phys. 11 (2013) 180.
[131] M. Gorbahn and U. Haisch, J. High Energy Phys. 06 (2014) 033.